Mater. Res. Soc. Symp. Proc. Vol. 845 © 2005 Materials Research Society AA6.2

New biological labels based on functionalized YVO_4:Eu nanoparticles

D. Giaume, V Buissette, K. Lahlil, T. Gacoin, J.-P. Boilot
Laboratory of Condensed Matter Physics
Ecole Polytechnique, route de Saclay, 91128 Palaiseau, France

D. Casanova, E. Beaurepaire, M.-P. Sauviat, A. Mercuri, A. Alexandrou
Laboratory for Optics and Biosciences, CNRS UMR 7645, INSERM U45L
Ecole Polytechnique, route de Saclay, 91128 Palaiseau, France

Abstract

Lanthanide-ion doped oxide (YVO_4:Eu) nanoparticles were synthesized as aqueous colloids and functionalized by a bioactive silane shell to be used as fluorescent biological labels. Nanoparticles functionalized with guanidinium groups were able to act as artificial toxins which specifically target Na^+ channels. They were individually detectable in live cardiac myocytes. Functionalized oxide nanoparticles appear as a new interesting tool, especially attractive for long-term single-molecule tracking due to their photo-stability and long luminescence lifetime.

Introduction

Fluorescent organic compounds have been extensively used for the visualization of the different components of biological systems.[1,2,3] Now, an interesting issue is to track labeled individual species during *in vitro* or *in vivo* experiments. The use of organic dyes is limited for that purpose because of their rapid photobleaching. A few years ago, it was suggested that functionalized inorganic CdSe nanocrystals could be used,[4,5] since they exhibit very good emission properties with the appropriate stability.[6,7,8,9,10] Moreover, the emission wavelength can be tuned by modifying the size of the particles.
In this paper, we discuss the application of a new promising class of biological fluorescent nanoparticles based on rare earth doped oxide nanocrystals. These compounds are characterized by high emission yields, at wavelengths that do not depend on the size of the particles, but which can be tuned by changing the chemical nature of the rare earth doping. Moreover, compared to CdSe particles, these systems do not exhibit any blinking of their emission since they are doped with a large number of emitting ions.
Our study is focused on europium doped yttrium vanadate (YVO_4:Eu) nanoparticles, with the aim to use them for the optical detection of Na^+ channel dynamics on cell membranes. These channels are essential elements for electrical signaling in the nervous, muscular, and cardiac systems. Our goal is to have a direct detection of the mobility of these channels in the bilayered membrane of the cell, by tracking luminescent nanoparticles that are selectively bound to them. Our work is divided into four steps : i) to achieve the synthesis of the nanoparticles and their functionalization so as to ensure a specific interaction with the Na^+ channels ii) to show the possibility of detection of individual particles iii) to test their bioactivity and iv) to visualize the nanoparticles *in situ* on cell membranes.

Synthesis and functionalization of the nanoparticles

The colloidal synthesis of YVO_4:Eu nanoparticles was described in details in a previous publication.[11,12] In a typical experiment, an aqueous solution of sodium orthovanadate (0.1 M) was added dropwise into an yttrium (III) nitrate solution (0.1 M) containing 10 molar % of europium (III) nitrate. The cloudy precipitate thus obtained was purified by dialysis, leading to a slightly diffusing suspension. The average diameter of the nanoparticles was around 40 nm as deduced from dynamic light scattering measurements (Fig. 1.a). X ray diffraction experiments performed on a dried powder of particles showed that they had the same crystalline structure as the bulk material prepared through usual high temperature processes. Electron microscopy images revealed that the particles had an ovoid shape and were mostly polycrystalline (Fig. 1.b). The surface functionalization of the particles consists in grafting an organic function that will determine the specific interactions between the particles and the sodium channels. It is well known that two natural toxins, tetrodotoxin (TTX) and saxitoxin (STX) selectively inhibit the Na^+ channels,[13] by plugging their guanidinium group into the channel mouth.[14,15] It could be expected that the grafting of guanidinium groups at the surface of the particles will provide the desired specific interactions.

Functionalization of the YVO_4:Eu nanoparticles was achieved by encapsulation with a thin shell of silane bearing the guanidinium groups (Fig. 1.c). Firstly, 10 equivalents of tetramethylammonium silicate (0.5 M) were added into the colloidal solution of particles to ensure the adsorption of silicate ions at the surface of the particles. The solution was purified by dialysis to remove all excess silicate ions. Then, a functionalized silicon alkoxide having epoxy groups (glycidoxypropyltrimethoxysilane) was polymerized around the particles through controlled hydrolysis/condensation reactions.[12] Preferential deposition of the silane at the surface of the particles was ensured by the silicate ions deposited at first. Unavoidable small clusters of polymerized silane can be removed by centrifugation of the suspension, leaving the clusters in the supernatant. The particles were then dispersed in a fresh water/ethanol mixture. NMR, Infra-red spectroscopy and thermogravimetric analysis of the particles showed that the particles were finally covered by a silica shell with a thickness of about 2 nm. Finally, guanidinium groups were covalently grafted at the surface of the silane shell through nucleophilic reaction of one of the amine functions of guanidine with the pending epoxy functions.

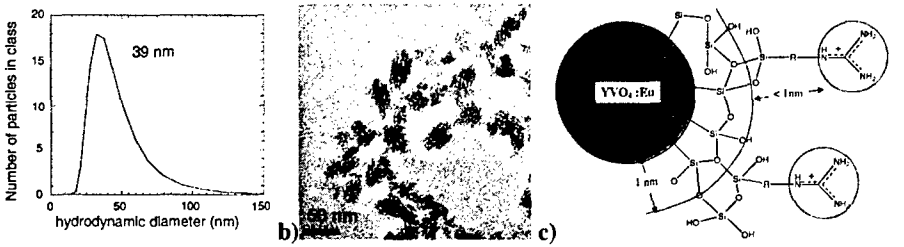

Figure 1. Size dispersion (**a**) and TEM image (**b**) of nanoparticles obtained by precipitation-redispersion. (**c**) scheme of a guanidine-functionalized nanoparticle. Guanidine functions have been circled.

Single nanoparticle detection through fluorescence microscopy measurements

Emission properties of the YVO_4:Eu nanoparticles are quite similar to the ones of the bulk material (Fig. 2.a). The emission spectrum consists in very narrow emission lines characteristic of the radiative transitions within the f electrons of the europium ions. The major contribution lies at 617 nm, and corresponds to the $^5D_0$-$^7F_2$ transition. The integrated emission yield is about 15-20%. The excitation spectrum consists in two distinct contributions. The first one is a broad band in the UV region, peaking at 280 nm. It corresponds to a V-O charge transfer absorption with a corresponding cross section of about 10^5 cm^{-1}. Following the absorption of a photon, energy transfer within the vanadate sub-lattice leads to the excitation of the emitting Eu ions. The other contribution in the excitation spectrum consists in narrow lines corresponding to the direct excitation of the europium ions through internal transitions within the f electrons. The most intense bands lie at 396 nm, 466 nm and 545 nm. The corresponding absorption cross section is rather low, a few cm^{-1}.

Fluorescence microscopy measurements were first achieved on nanoparticles deposited on a glass substrate, using an inverted microscope under wide-field illumination. Excitation of the luminescence of the particles was performed using the 465.8 nm line of an Ar^+ laser, while the detection of the emission was achieved on a CCD camera after filtering of the emitted light at 617 nm with an interferential filter.[16]

Fig. 2.b shows the image obtained using an incident excitation power of 2.4 kW/cm^2 and an integration time of 100 ms. Bright spots are clearly visible, but strong variations of intensity can be noticed. As the emission intensity is proportional to the volume of the nanoparticles, these variations can then be due either to aggregates of different numbers of particles or to the size dispersion of individual nanoparticles. To answer this question, a quantitative analysis of the distribution of emission intensities was carried out. The same fluctuations were observed by diluting the colloidal solution, although it should limit the aggregation of the particles. Moreover, a very good correlation was observed when comparing statistics of the number of photons emitted by one spot and the size dispersion of the nanoparticles as determined from electron microscopy imaging. We can then conclude that each spot corresponds to a unique particle.

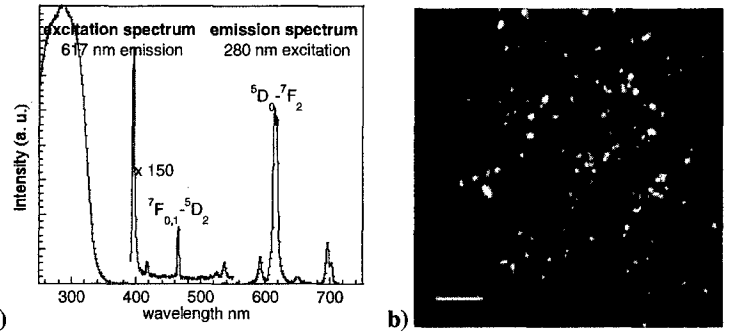

Figure 2. (a) (250-550 nm) excitation spectrum for an emission wavelength of 617 nm and (550-750 nm) emission spectrum for an excitation wavelength of 280 nm of 39 nm YVO_4:Eu nanoparticles **(b)** Fluorescence image of nanoparticles spin-coated on a glass coverslip. Scalebar : 5 µm

Biological activity

We studied the effect of the functionalized nanoparticles on quiescent frog heart auricular tissue and recorded action potentials (AP) at 20 °C by means of intracellular microelectrode techniques used in the floating mode.[17,18] In the Ringer* solution, the atrial AP is characterized by a rapid upstroke involving a fast Na^+ influx followed by a plateau carried by a Ca^{2+} influx while a K^+ efflux repolarizes the membrane (Fig. 3.a). The maximum upstroke velocity of the AP (V_{max}), i.e. the maximum rate of depolarization, was used as an index of the Na^+ conductance, G_{Na}[19] (Fig. 3.b). Addition of unfunctionalized nanoparticles (in the dose range of 10^9 to 10^{11} nanoparticles/ml) or guanidinium ions (at concentrations ranging from 0.1 nM to 1 mM) to the Ringer solution does not significantly affect AP and V_{max}. The application of a Ringer solution containing functionalized nanoparticles (5 µL/ml, corresponding to a concentration of 0.8 mM in VO_4^{3-} ions) to the auricle does not modify the amplitude of the AP but decreases V_{max} (Fig. 3.c and d). The inhibition of V_{max} induced by the functionalized nanoparticle solution is dose-dependent (see Fig. 4). Thus, the guanidinium groups at the surface of the particles do have a blocking effect on Na^+ channels as in the case of STX, so that functionalized nanoparticles behave as artificial toxins.

In vivo studies on cell membrane

Fluorescence microscopy was performed on single cardiac myocytes obtained by enzymatic dissociation of the isolated frog auricle.[18] Two groups of myocytes were imaged: a control group of unlabeled myocytes and a nanoparticle-labeled group of myocytes incubated for 5 min in a Ringer solution containing 10^{11} functionalized nanoparticles/ml and then carefully rinsed with a Ringer solution without nanoparticles to remove unattached nanoparticles. Only nanoparticle-labeled myocytes presented bright spots (Fig. 5. b) indicating the presence of individual nanoparticles on the cell membrane.

In order to check the specificity of the interaction between the nanoparticles and the Na^+ channels, we first applied STX (15 nM, a concentration that blocks more than 90% of the Na^+ channels) for 5 min to myocytes. We then added the solution containing 10^{11} nanoparticles/ml to the Ringer solution containing STX and, after 5 min, rinsed the cells with pure Ringer solution. No nanoparticles were observed on the cells after this treatment (Fig. 5.d), which indicates that saturating the Na^+ channels by STX prevents nanoparticle binding.

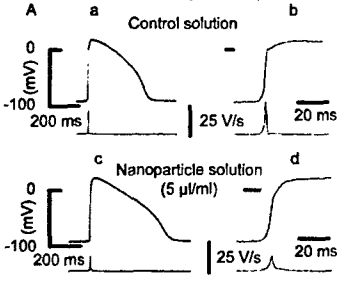

Figure 3. Typical action potential (upper traces) and V_{max} (lower traces) recorded on the same auricle at fast (a and c) and slow (b and d) sweep speed : Ringer solution (a and b); Ringer solution containing a nanoparticle solution (5 µl/ml) (c and d)

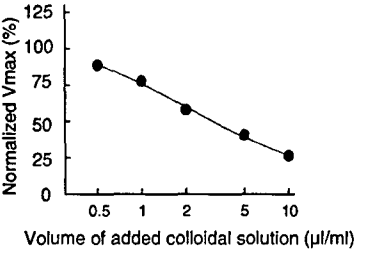

Figure 4. Dose-dependent effect of functionalized nanoparticles on Vmax.

This experiment demonstrates that nanoparticles bind to Na^+ channels and do not exhibit non-specific binding on cell membranes.
As it is usually done in single-molecule experiments, the images shown in Figs. 5.b and 5.d were obtained after prior illumination of the cells during a few seconds in order to photobleach their endogenous fluorescence. However, lanthanide luminescence is characterized by long excited-state lifetimes (0.7 ms for nanoparticles) which can be exploited to obtain single-molecule images even in the presence of strong cell fluorescence (Fig. 5). For this purpose, we implemented a simple time-gated detection scheme using two synchronized mechanical choppers. The first chopper modulates the laser beam, while the second is placed before the CCD detector. Photon collection is started 10-80 μs after stopping the excitation, which eliminates both the scattered laser light and the short-lived (~ns) cellular fluorescence. Figs. 5.e and 5.f present images obtained without any pre-bleaching of the cells. In the absence of time-gating (Fig. 5.e), direct detection of single nanoparticles is not possible because of cell fluorescence (15000-50000 photons/pixel/s). In contrast, time-gated detection (Fig. 5.f) allows a clear observation of single nanoparticles (peak signal 200 photons/pixel/s) despite strong cellular fluorescence. Residual background light in Fig. 5.f is essentially caused by nanoparticles present in out-of-focus planes. Fig. 5.f shows a heterogeneous distribution of Na^+ channels in cardiac myocytes.

Conclusion

This new class of fluorescent probes is based on oxide nanoparticles doped with rare-earth ions. They are especially suitable for long-term single-molecule tracking, due to their photo-stability, absence of emission intermittency and their long fluorescence lifetime. We have demonstrated specific targeting and imaging of Na^+ channels in frog live cardiac myocytes using individual detection of these nanoparticles.
The functionalization described here is easily adaptable to other biological species. In addition to channel diffusion and clustering, this fluorescent label opens up possibilities for studying the long-term diffusion dynamics and the fate of receptors, signaling complexes, and pathological agents in cells and tissues.

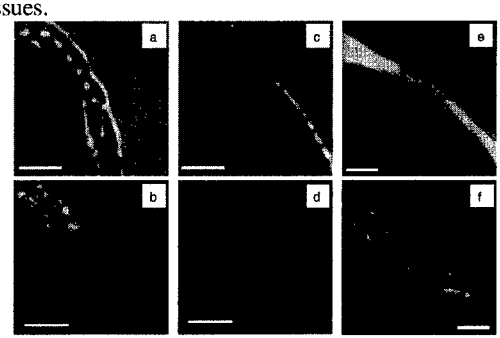

Figure 5. Frog live cardiac myocytes bathed in Ringer solution labeled with functionalized nanoparticles (30 nm, 20% doped) (a and b) or with saxitoxin (c and d). (a) and (c) Transmitted white-light images of the two different cells. (b) and (d) Wide-field fluorescence microscopy images. (e) and (f) functionalized nanoparticles (10^{11} nanoparticles/ml) observed without pre-bleaching cell fluorescence. (e) without time-gated detection; (f) with time-gated detection. Intensity at the sample : 5 kW/cm^2; integration time: 1 s; scale bar: 5 μm.

[1] Zhang, J.; Campbell, R. E.; Ting, A. Y.; Tsien, R. Y. *Nat. Rev. Mol. Cell Biol.* **2002**, *3*, 906-918.
[2] Haugland, R. P. *Handbook of Fluorescent Probes and Research Products*; Molecular Probes: Eugene, OR, 2002.
[3] Charpak, S.; Mertz, J.; Beaurepaire, E.; Moreaux, L.; Delaney, K. *Proc. Nat. Acad. Sci. USA* **2001**, *98*, 1230-1234.
[4] Bruchez, M.; Moronne, M.; Gin, P.; Weiss, S.; Alivisatos, A. P. *Science* **1998**, *281*, 2013.
[5] Chan, W. C. W.; Nie, S. *Science* **1998**, *281*, 2016.
[6] Dubertret, B.; Skourides, P.; Norris, D. J.; Noireaux, V.; Brivanlou, A. H.; Libchaber, A. *Science* **2002**, *298*, 1759.
[7] Dahan, M.; Lévi, S.; Luccardini, C.; Rostaing, P.; Riveau, B.; Triller, A. *Science* **2003**, *302*.
[8] Wu, X.; Liu, H.; Liu, J.; Haley, K. N.; Tradway, J. A.; Larson, J. P.; Ge, N.; Peale, F.; Bruchez, M. P. *Nature Biotech.* **2003**, *21*, 41.
[9] Jaiswal, J. K.; Mattousi, H.; Mauro, J. M.; Simon, S. M. *Nature Biotech.* **2003**, *21*, 47.
[10] Kim, S.; Lim, Y. T.; Soltesz, E. G.; Grand, A. M. D.; Lee, J.; Nakayama, A.; Parker, J. A.; Mihaljevic, T.; Laurence, R. G.; Dor, D. M.; Cohn, L. H.; Bawendi, M. G.; Frangioni, J. V. *Nature Biotech.* **2004**, 22, 93-97.
[11] Huignard, A.; Gacoin, T.; Boilot, J.-P. *Chem. Mat.* **2000**, *12*, 1090.
[12] Huignard, A.; Gacoin, T.; Chaput, F.; Boilot, J.-P. *Mat. Res. Soc. Symp. Proc.* **2001**, *667*, G.4.5.1.
[13] Narahashi, T. *J. Pharmacol. Exp. Ther.* **2000**, *294*, 1.
[14] Hille, B. *Biophys. J.* **1975**, *15*, 615-619.
[15] Kao, C. Y. *Ann. N. Y. Acad. Sci.* **1986**, *479*, 52-67.
[16] Beaurepaire, E.; Buissette, V.; Sauviat, M.-P. ; Giaume, D. ;Lahlil, K. ;Mercuri, A. ;Casanova, D. ; Huignard, A. ; Martin, J.-L. ; Gacoin, T. ; Boilot, J.-P. ; Alexandrou, A. ; *Nanoletters* **2004**, *4(11)*, 2079-2083.
[17] Sauviat, M.-P.; Marquais, M.; Vernoux, J.-P. *Toxicon* **2002**, *40*, 1155-1163.
[18] Sauviat, M.-P.; Colas, A.; Pages, N. *BioMed Central Pharmacology* **2002**, 2, 15.
[19] Sheets, M. F.; Hanck, D. A.; Fozzard, H. A. *Circ. Res.* **1989**, *65*, 1462-1465.

* The composition of the physiological Ringer solution was (mM): NaCl: 1103.5; KCl: 2.5; Ca Cl_2: 2; $MgCl_2$: 1; Na^+ pyruvate: 5; HEPES (NaOH): 10; glucose: 10; albumine: 1 mg/ml; pH: 7.34.